UNIVERSIDADE DE SÃO PAULO

Numerical simulation of viscous fluid:

buckling of planar jets

MURILO F. TOME; SEAN MCKEE

Nº 007

NOTAS

Instituto de Ciências Matemáticas de São Carlos

Instituto de Ciências Matemáticas de São Carlos

ISSN - 0103-2577

Numerical simulation of viscous fluid: buckling of planar jets

MURILO F. TOME; SEAN MCKEE

Nº 007

N O T A S D O I C M S C
Série Computação

São Carlos
mar. / 1994

Numerical Simulation of Viscous Fluid: Buckling of Planar Jets

Murilo F. Tome

ICMSC - USP de São Carlos

Departamento de Ciência da Computação e Estatistica

Av. Dr. Carlos Botelho, 1465 - Caixa Postal 668

13560-970 - São Carlos - SP - Brazil

and

Sean McKee

University of Strathclyde

Department of Mathematics

26 Richmond street - Livingstone Tower

Glasgow G1 1XH - U. K.

Abstract

The phenomenon of viscous fluid buckling has been the subject of study by various investigators in recent years. In particular, Cruickshank[6] and Tchavdarov, Yarin and Radev[7] have presented theoretical results for predicting the buckling of a thin jet. However, these models are based on a one-dimensional analysis and consequently can only hope to approximate the phenomenon. In this paper we present a two-dimensional calculation using the full Navier-Stokes equations, but omitting surface tension. The computation is performed using the GENSMAC code and the results agree well qualitatively with the experimental and theoretical results presented by Cruickshank and Munson[5] and Cruickshank[6] respectively.

1. INTRODUCTION

It is well known that the Euler equations govern the critical load for elastic buckling in slender columns with given end conditions. However, a similiar phenomenon is also observed in viscous fluids and as yet no similar satisfactory mathematical theory exists to describe the phenomenon. It manifests itself by the coiling or folding of a thin stream onto a flat plate just as honey does "falling" from a spoon.

Taylor[1] was the first to study this phenomenon qualitatively. Then followed a number of related papers, for example Lienhard[2], Suleiman and Munson[3], before an extensive experimental examination of jet buckling was carried out by Cruickshank[4] - see also Cruickshank and Munson[5]. Approximate mathematical models have been developed by Cruickshank[6] and Tchavdarov, Yarin and Radev[7] and have been shown not to compare too badly with experiments. An exhaustive bibliograph can be found in the review article by Bejan[8].

The viscous jet may be either in tension or compression, depending on the velocity gradient along its axis (Cruickshank and Munson[5]). If the diameter of the jet increases in the downstream direction, the viscous normal stress along its axis is one of compression. If this viscous compressive component of the normal stress is large enough, the net axial stress in the jet may be compressive. Thus, near the flat plate, sufficiently large axial compressive stresses along with a sufficiently 'slender' jet combine, under appropriate circumstances, to produce the fluid mechanics analogue to the buckling of a slender solid column.

The purpose of this paper is to demonstrate that, by solving the full two-dimensional Navier-Stokes equations, this buckling phenomenon can be simulated and that despite the fact that surface tension is neglected in the numerical experiments the results agree qualitatively with those of Cruickshank and Munson[5] and Cruickshank[6]. The computation is performed by the GENSMAC code for which we present a brief description. Details of the methodology employed can be found in Tome[9] and Tome and McKee[10].

2. BRIEF DESCRIPTION OF THE GENSMAC CODE

The GENSMAC code solves the two-dimensional time-dependent Navier-Stokes equations for an incompressible viscous fluid. It is an updated version of the SMAC (Simplified Marker-and-Cell) method (Amsden and Harlow[11]) for calculating time-dependent free-surface flow problems employing pressure and velocity as the primary dependent variables. It employs a finite difference approach on a staggered grid. An adaptive time-stepping technique has been used and a conjugate gradient solver is employed to invert the discrete Poisson equation. The code is designed to deal with free surface flows within a general domain with free-slip or no-slip rigid boundaries. A number of inflows and outflows can be handled as can any number of internal obstacles.

2.1. *Basic Equations*

The basic equations are the two-dimensional Navier-Stokes equations together with the mass conservation equation which in non-dimensional form can be written as

$$\begin{aligned}
\frac{\partial u}{\partial t} + \frac{\partial u^2}{\partial x} + \frac{\partial uv}{\partial y} &= -\frac{\partial p}{\partial x} + \left(\frac{1}{Re}\right)\frac{\partial}{\partial y}\left(\frac{\partial u}{\partial y} - \frac{\partial v}{\partial x}\right) + \frac{1}{F_r^2}g_x \\
\frac{\partial v}{\partial t} + \frac{\partial uv}{\partial x} + \frac{\partial v^2}{\partial y} &= -\frac{\partial p}{\partial y} - \left(\frac{1}{Re}\right)\frac{\partial}{\partial x}\left(\frac{\partial u}{\partial y} - \frac{\partial v}{\partial x}\right) + \frac{1}{F_r^2}g_y \\
\frac{\partial u}{\partial x} + \frac{\partial v}{\partial y} &= 0
\end{aligned}$$

where $Re = UL/\nu$ and $F_r = U/\sqrt{Lg}$ are the associated Reynolds number and Froude number respectively. U and L are typical velocity and length scales and ν is the kinematic viscosity, g is the gravitational constant with $\mathbf{g}(\mathbf{x}) = (g_x, g_y)^T$ the unit gravitational field vector, $\mathbf{u} = (u, v)^T$ are the non-dimensional components of velocity while p is the non-dimensional pressure per unit density.

2.2. *Solution Procedure*

It is supposed that at a given time t_0, the velocity field $\mathbf{u}(\mathbf{x}, t_0)$ is known and boundary conditions for velocity and pressure are given. The updated velocity field $\mathbf{u}(\mathbf{x}, t)$, at $t = t_0 + \delta t$ is calculated as follows:

1. Let $\tilde{p}(\mathbf{x}, t_0)$ be a pressure field which satifies the correct pressure condition on the free surface.

2. Calculate the intermediate velocity field $\tilde{\mathbf{u}}(\mathbf{x}, t)$ from the explicit discretised form of

$$\begin{aligned}
\frac{\partial \tilde{u}}{\partial t} &= \left[-\frac{\partial u^2}{\partial x} - \frac{\partial uv}{\partial y} - \frac{\partial \tilde{p}}{\partial x} + \left(\frac{1}{Re}\right)\frac{\partial}{\partial y}\left(\frac{\partial u}{\partial y} - \frac{\partial v}{\partial x}\right) + \frac{1}{F_r^2}g_x\right]_{t=t_0} \\
\frac{\partial \tilde{v}}{\partial t} &= \left[-\frac{\partial uv}{\partial x} - \frac{\partial v^2}{\partial y} - \frac{\partial \tilde{p}}{\partial y} - \left(\frac{1}{Re}\right)\frac{\partial}{\partial x}\left(\frac{\partial u}{\partial y} - \frac{\partial v}{\partial x}\right) + \frac{1}{F_r^2}g_y\right]_{t=t_0}
\end{aligned}$$

where $\tilde{\mathbf{u}}(\mathbf{x}, t_0) = (u, v)^T$ using the correct boundary conditions for $\mathbf{u}(\mathbf{x}, t_0)$. The intermediate velocity field is then corrected by

$$\mathbf{u}(\mathbf{x}, t) = \tilde{\mathbf{u}}(\mathbf{x}, t) - \nabla\psi$$

with

$$\nabla^2\psi = \nabla.\tilde{\mathbf{u}}(\mathbf{x}, t).$$

Thus, $\mathbf{u}(\mathbf{x}, t)$ now satisfies

$$\nabla.\mathbf{u}(\mathbf{x}, t) = 0.$$

3. Solve the Poisson equation

$$\nabla^2\psi = \nabla.\tilde{\mathbf{u}}(\mathbf{x}, t)\ .$$

4. Compute the velocity

$$\mathbf{u}(\mathbf{x}, t) = \tilde{\mathbf{u}}(\mathbf{x}, t) - \nabla\psi\ .$$

5. Compute the pressure

$$p = \tilde{p} + \frac{\psi}{\delta t}\ .$$

2.3. *Boundary Conditions*

There are several types of boundary conditions which can be applied at the boundary, namely: no-slip, free-slip, prescribed inflow, prescribed and continuative outflow. Except for the no-slip condition, these prescriptions resemble those considered by the SMAC method. For a detailed discussion see Tome [9]. On the mesh boundary, the apropriate boundary condition for the Poisson equation (Amsden and Harlow[11]) is

$$\frac{\partial\psi}{\partial n} = 0\ .$$

2.4. *Free Surface Stress Conditions*

The appropriate free-surface boundary conditions are the vanishing of the normal and tangential stresses which in differential form take the form (Hirt and Shannon[12])

$$p - (2/Re)\left[n_x^2\frac{\partial u}{\partial x} + n_x n_y\left(\frac{\partial u}{\partial y} + \frac{\partial v}{\partial x}\right) + n_y^2\frac{\partial v}{\partial y}\right] = 0$$

$$(1/Re)\left[2n_x m_x\frac{\partial u}{\partial x} + (n_x m_y + n_y m_x)\left(\frac{\partial u}{\partial y} + \frac{\partial v}{\partial x}\right) + 2n_y m_y\frac{\partial v}{\partial y}\right] = 0$$

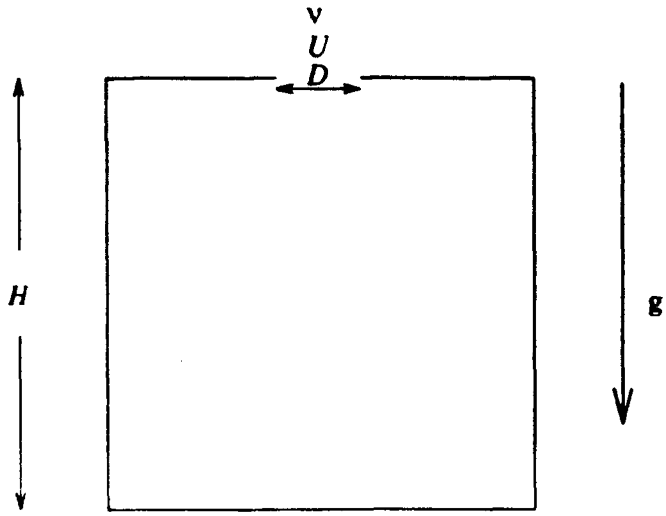

Fig. 1.

respectively, where n and m are the normal and tangential directions to the surface respectively. These conditions are applied by making local finite differences approximations on the free surface.

2.5. *Marker-Particles*

Marker particles are used to represent the fluid itself. Their essential task is to provide the position of the moving free surface so that the stress conditions can be applied accurately. They are updated at the end of each calculational time-step so as to provide the dynamics of the fluid motion.

The new particle coordinates are found by solving

$$\frac{dx}{dt} = u \qquad \text{and} \qquad \frac{dy}{dt} = v$$

using Euler's method. Thus, after the velocity field is updated, the particles are moved according to

$$x_p^{n+1} = x_p^n + u_p \delta t^{n+1}$$

$$y_p^{n+1} = y_p^n + v_p \delta t^{n+1}$$

where (x_p^n, y_p^n) is the current particle position , δt^{n+1} is the actual time-step employed and (x_p^{n+1}, y_p^{n+1}) its updated position.

The velocities u_p, v_p are found from a bilinear approximation using the four nearest u, v velocities.

TABLE I

H/D	D \ U	ν = 0.005 m^2/s		ν = 0.010 m^2/s	
		0.5 m/s	1.0 m/s	0.5 m/s	1.0 m/s
16.7	3 mm	Re = 0.30 F_r = 2.914 **B**	Re = 0.60 F_r = 5.829 **nB**	Re = 0.15 F_r = 2.914 **B**	Re = 0.30 F_r = 5.829 **B**
12.5	4 mm	Re = 0.40 F_r = 2.524 **nB**	Re = 0.80 F_r = 5.048 **nB**	Re = 0.20 F_r = 2.524 **B**	Re = 0.40 F_r = 5.048 **nB**
10.0	5 mm	Re = 0.50 F_r = 2.257 **nB**	Re = 1.00 F_r = 4.515 **nB**	Re = 0.25 F_r = 2.257 **nB**	Re = 0.50 F_r = 4.515 **nB**

B: jet buckled; **nB**: jet did not buckle.

3. JET BUCKLING: A Numerical Experiment

The experimental results of Cruickshank and Munson[5] suggest that buckling will occur when the Reynolds number (Re) averages about 0.56 or less. A pertubation analysis of Cruickshank[6] suggests that the plate-orifice distance for buckling is given by

$$H/D = (2n + 1)\pi \qquad (n = 0, 1, \cdots) .$$

Here D and H are the slit width and the height of the inlet to the plate respectively. Experimental evidence, provided by Cruickshank and Munson[5], then leads Cruickshank[6] to suggest that buckling of a planar jet appears to occur when $n = 1$, that is, when H/D is greater than 3π.

Based on these assumptions a series of runs were performed using the GENSMAC code in order to make a comparison with experimental results. The following numerical experiment was carried out.

We considered an empty square cavity with the no-slip condition imposed on its walls. Through an inlet a thin jet of fluid is injected into the cavity at a constant velocity. The cavity is chosen to be sufficiently wide to permit buckling, when it occurs, without the jet touching the cavity walls. The geometry of the experiment is shown in Fig. 1, where again D is the inlet size and H is the height of inlet jet to the bottom wall of the cavity. The value of H was held fixed while the three other parameters: inlet size D, inlet velocity U and the kinematic viscosity ν, assumed several values within the runs. The following data were employed:

$$D = 3,\ 4,\ 5\ [mm]$$
$$U = 0.5,\ 1.0\ [m/s]$$
$$\nu = 0.005,\ 0.010\ [m^2/s]$$

These gave 12 runs with a Reynolds number Re, based on the slit width, in the range of $[0.15, 1.0]$ and $(1/F_r^2)$ in the range $[0.0294,\ 0.1962]$. The height H was 5 cm in which case the ratio H/D took the values: 16.67 (D = 3 mm), 12.5 (D = 4 mm) and 10.0 (D = 5 mm). These were the only parameters which differed from one run to the next. The results are displayed in Table 1. Fig. 2 displays a particular buckling obtained for the data $D = 4\ mm$, $U = 0.5\ m/s$ and $\nu = 0.010\ m^2/s$ ($Re = 0.20$ and $H/D = 12.5$). Results for a jet which shows no signs of buckling are displayed in Fig. 3 for the data $D = 4\ mm$, $U = 0.5\ m/s$ and $\nu = 0.005\ m^2/s$ ($Re = 0.4$ and $H/D = 12.5$).

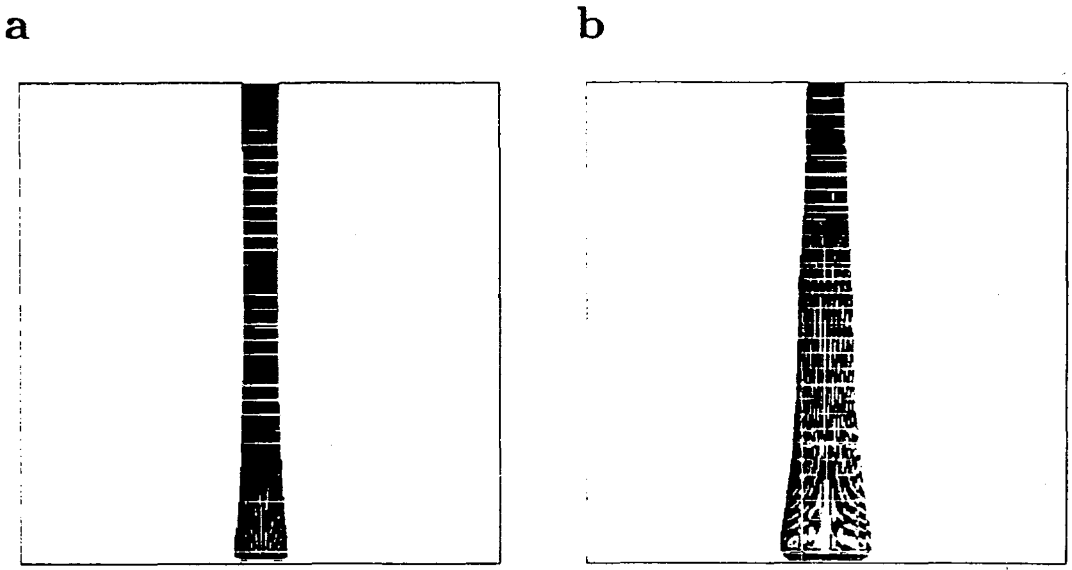

$Re = 0.20$. $F_r = 2.523$. $H/D = 12.5$

Fig. 2. Buckling jet.

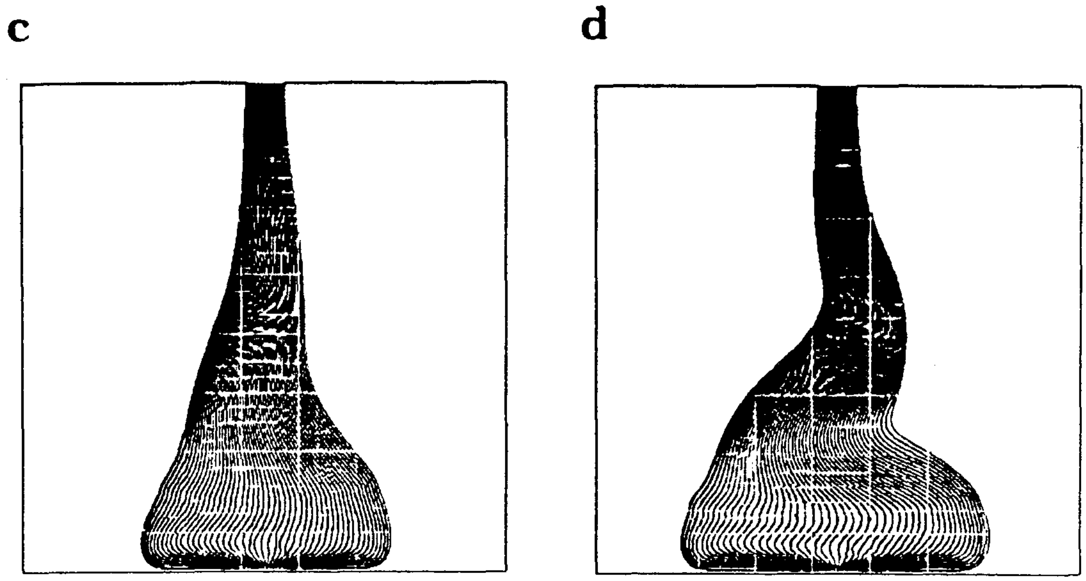

Fig. 2. Continued.

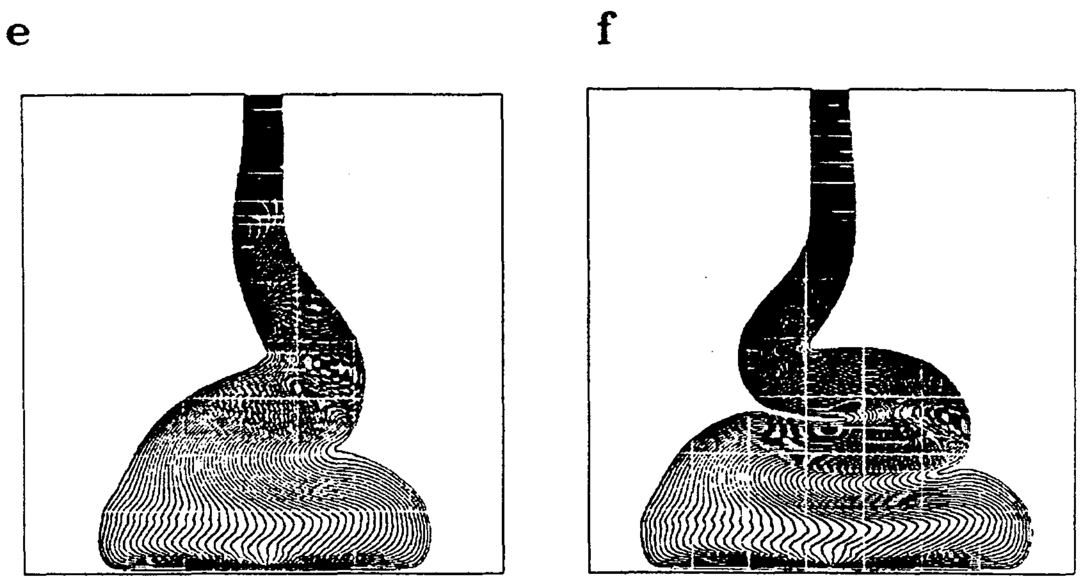

Fig. 2. Continued.

g h

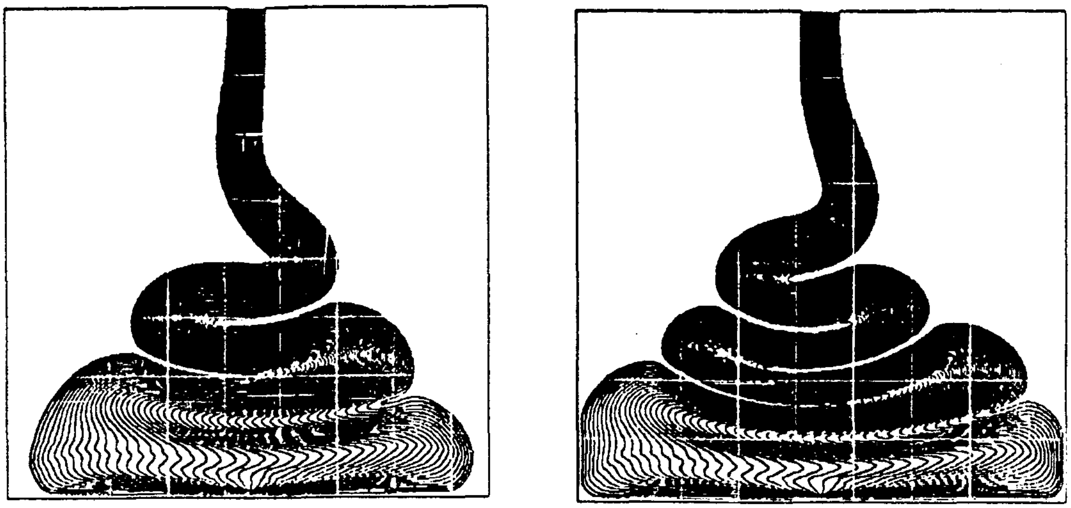

Fig. 2. Continued.

a b

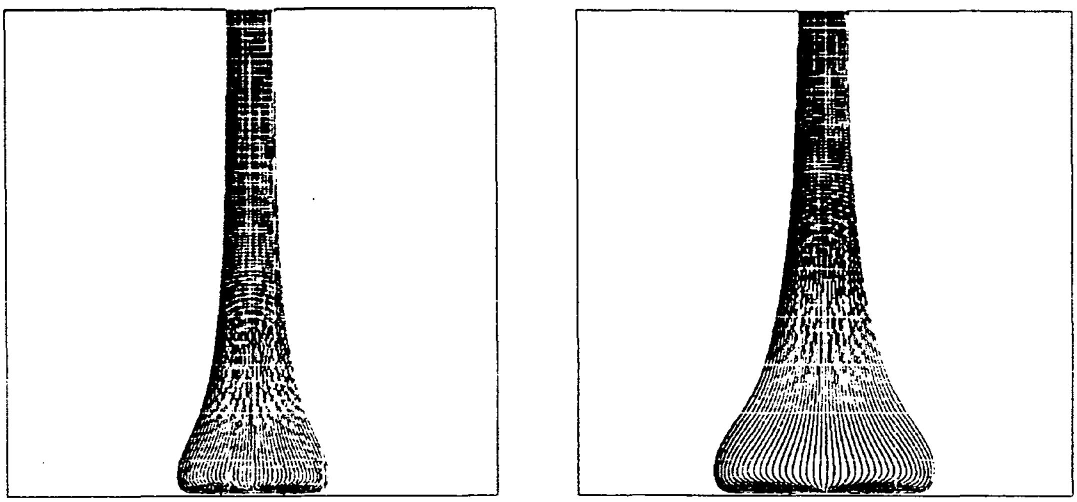

$Re = 0.40,\ F_r = 5.048,\ H/D = 12.5$

Fig. 3. Jet did not Buckle.

c d

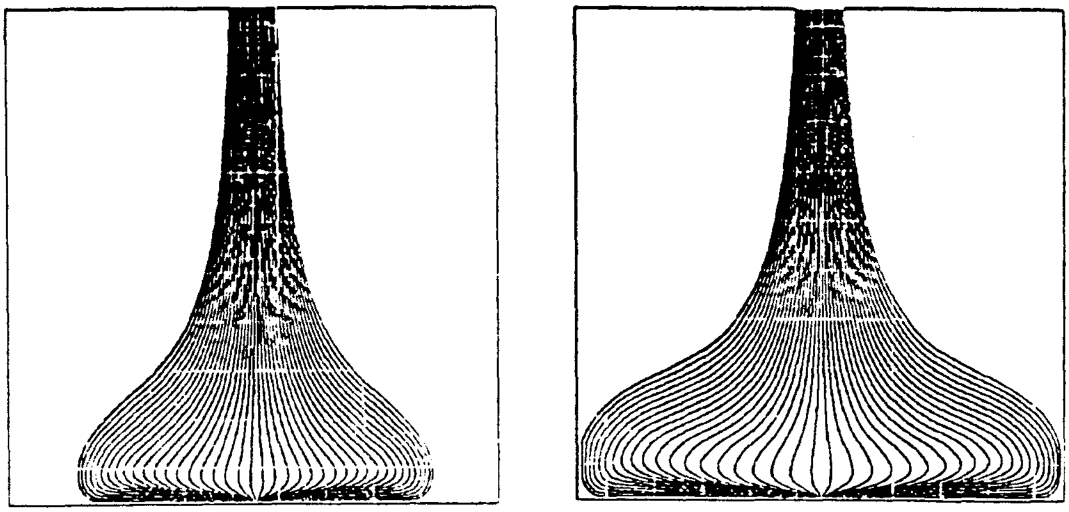

Fig. 3. Continued.

As we can see from Table I, the Reynolds number is an important factor in the buckling phenomenon. It can be observed that for $Re > 0.56$ buckling does not occur. However, for $Re = 0.4$, 0.5 buckling also did not occur. This, we believe, can be attributed to the fact that surface tension has been neglected in the numerical experiment, although it may be that H/D is not sufficiently large since this appears to be a dominant factor. To emphasize this point we consider the cases $Re = 0.5$, $F_r = 2.257$, $H/D = 10.0$ and $Re = 0.25$, $F_r = 2.257$, $H/D = 10.0$ which do not produce buckling but is close to the border of the buckling region, and perform two reruns with H/D equal to 16.0 and 14.0 respectively. In these runs the Reynolds numbers were 0.5 and 0.25 respectively. Both showed that the jet buckled; the results for the case $H/D = 16.0$ and $Re = 0.5$ are displayed in Fig. 4. These results are particularly interesting displaying different features from Fig. 2. For instance, both Figs. 2 and 4 display jet thinning although this very much more pronounced in Fig. 4, possibly due to the smaller Froude number. Also the fluid jet in Fig. 2 shows more clearly thickening moving back up the fluid jet prior to buckling. This effect was reported by Cruickshank and Munson[5]. Finally, Fig. 4 shows the fluid buckling to the right whereas in figure 2 the fluid buckles to the left. This illustrates a general point: that the fluid has no propensity to buckle in any preferred direction.

a

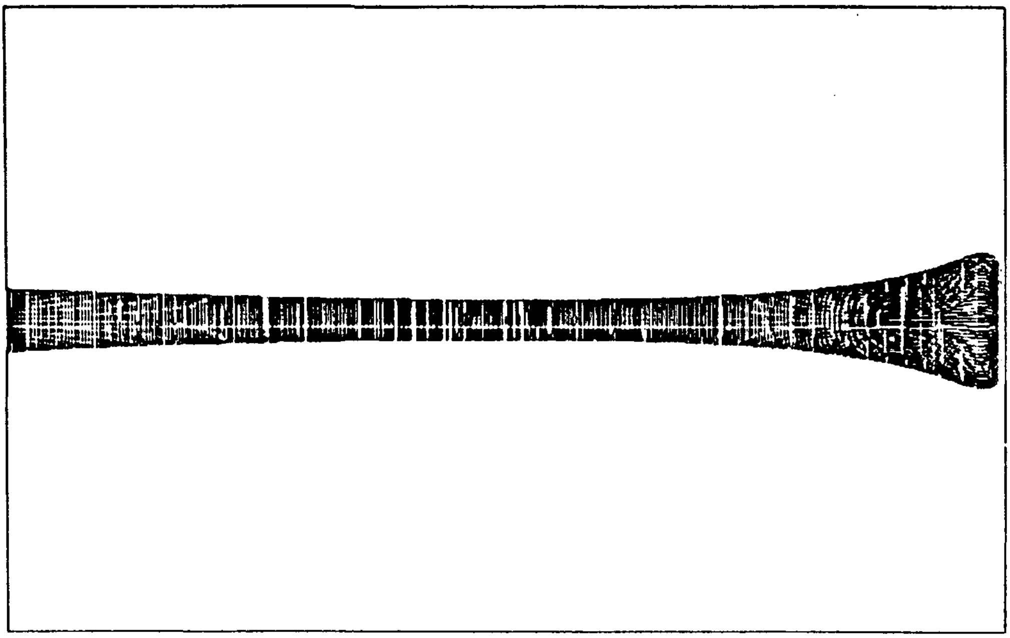

$Re = 0.5,\ F_r = 2.257,\ H/D = 16.0)$

Fig. 4. Buckling jet.

b

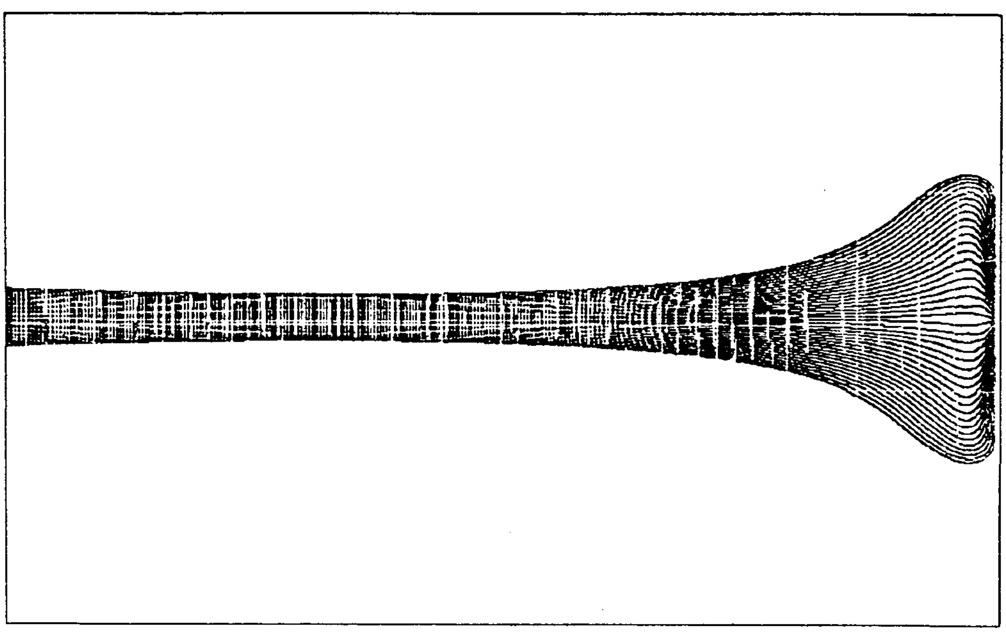

Fig. 4. Continued.

c

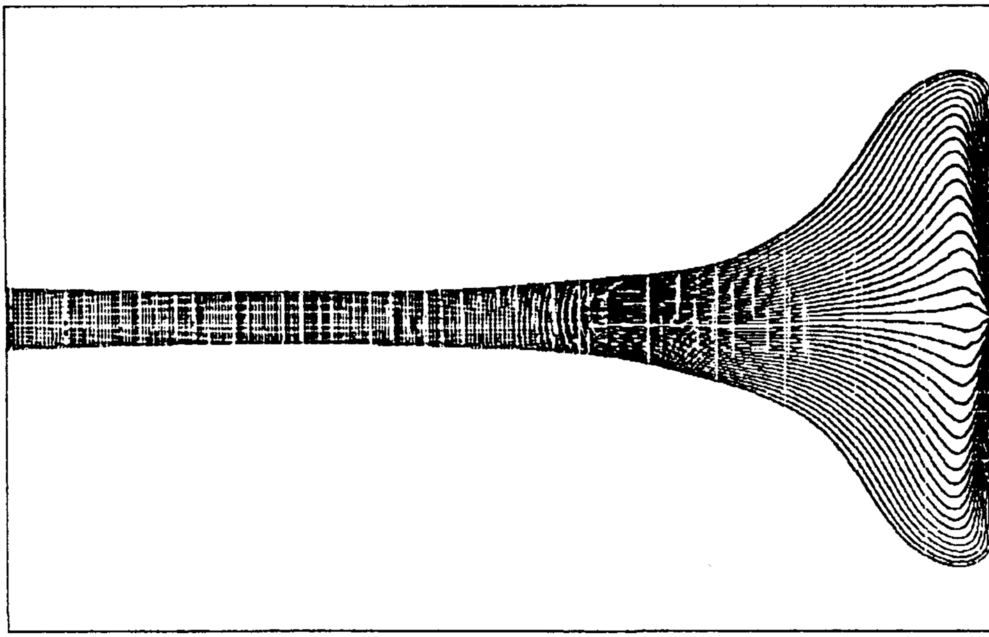

Fig. 4. Continued.

d

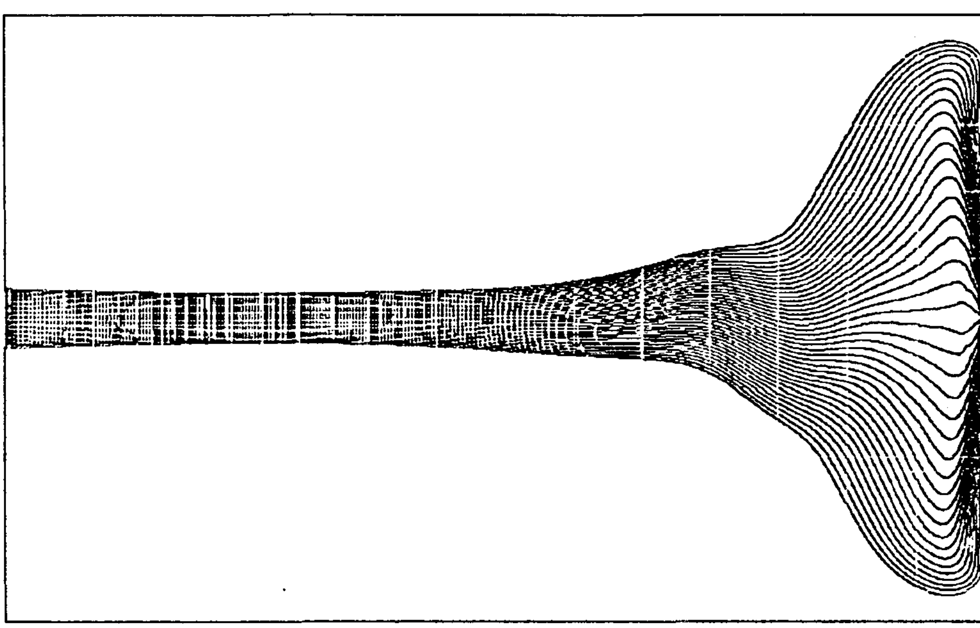

Fig. 4. Continued.

e

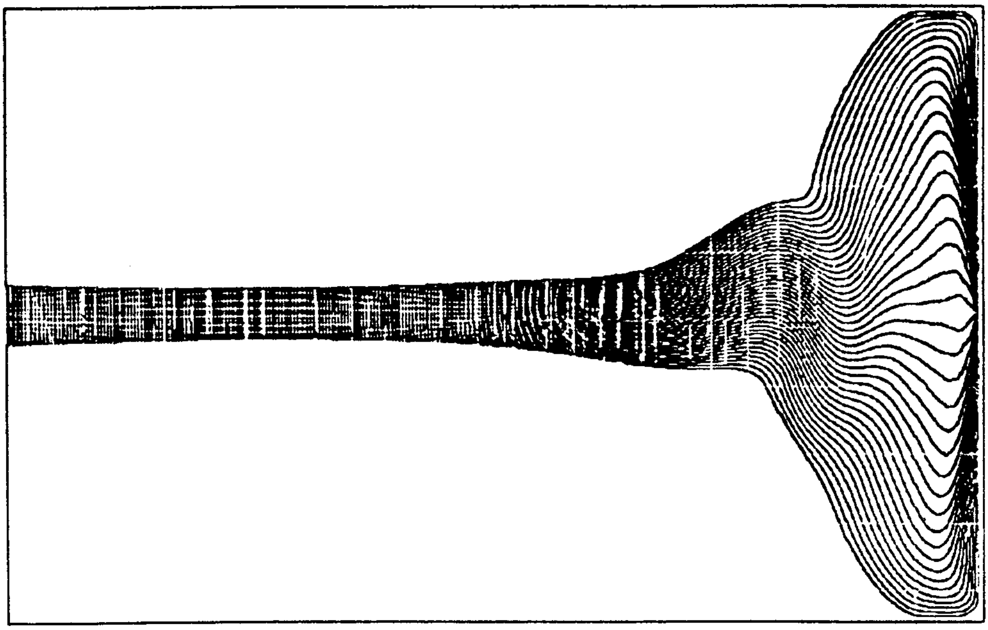

Fig. 4. Continued.

f

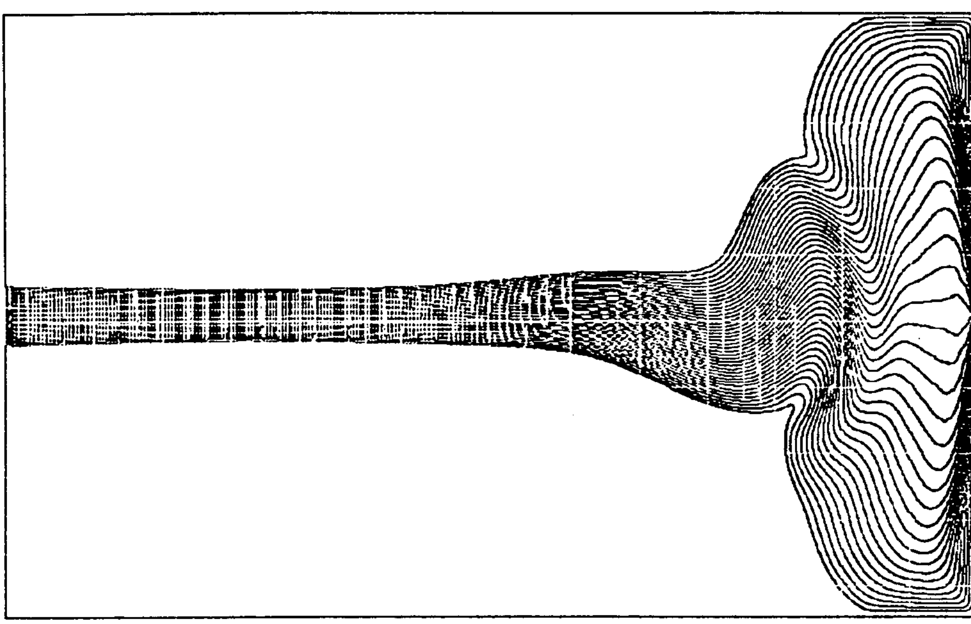

Fig. 4. Continued.

4. CONCLUDING REMARKS

This paper has been concerned with the use of the code GENSMAC to simulate the viscous buckling of a planar jet. The flow visualisation show good qualitative agreement with existing experimental results. This provides further evidence that GENSMAC is capable of simulating complicated free surface flow problems and illustrate certain features of viscous jet buckling: the lack of a preferred buckling direction and jet thickening and thinning.

ACKNOWLEDGMENTS

The authors wish to thank Dr. B. Duffy and Dr. S. Wilson of Department of Mathematics of University of Strathclyde for helpful discussions during the preparation of this work. The authors also wish to thank Dr. J. Crilly of Unilever Research for introducing us to this problem. The first author would like to acknowledge the financial support provided by the Brazilian funding agencies: CNPq - Conselho Nacional de Desenvolvimento Cientifico and FAPESP - Fundação de Amparo a Pesquisa do Estado de São Paulo.

REFERENCES

[1]G. I. Taylor, Instability of jets, threads and sheets of viscous fluids, Proc. Int. Congr. Appl. Mech., Berlin: Springer-Verlag. 1968..

[2]J. H. Lienhard, Capillary action in small jets impinging on liquid surfaces, J. Basic Eng. (Trans. of ASME) 1968, 137.

[3]S. M. Suleiman and B. R. Munson, *Phys. Fluids*, **24** (1981), 1.

[4]J. O. Cruickshank, Ph.D. dissertation, Iowa State University, Ames, Iowa, 1980.

[5]J. O. Cruickshank and B. R. Munson. *J. Fluid Mech.*. **113** (1981), 221.

[6]J. O. Cruickshank. *J. Fluid. Mech.*. **193** (1988), 111.

[7]B. Tchavdarov, A. L. Yarin and S. Radev. *J. Fluid Mech.*, **253** (1993), 593.

[8]A. Bejan, *Ann. Rev. Numer. Fluid Mech. Heat Transfer*, **1** (1987), 262.

[9]M. F. Tome, Ph.D. thesis. University of Strathclyde. Glasgow, UK, 1993.

[10]M. F. Tome and S. McKee, J. Comp. Phys., to appear, 1994.

[11]A. A. Amsden and F. H. Harlow, "The SMAC Method: A Numerical Technique for Calculating Incompressible Fluid Flows", Los Alamos Scientific Lab. Report LA-4370, Los Alamos, New Mexico, 1970.

[12]C. W. Hirt and J. P. Shannon, *J. Comp. Phys.*, **2** (1968), 403.

NOTAS DO ICMSC

Serie computaçao

Nº 007/94 TOME, M.F.; MCKEE, S. Numerical simulation of viscous fluid: buckling of planar jets

Nº 006/94 MASIERO, P.C.; OLIVEIRA, M.C.F.; GERMANO, F.S.R; PIERRI, G. Authoring and searching in dynamically growing hypertext data bases

Nº 005/94 NICOLETTI, M.C.; MONARD, M.C. Limiting the background knowledge in inductive logic programming

Nº 004/93 NICOLETTI, M.C.; MONARD, M.C. Learning horn clauses using the ILP system GOLEM

Nº 003/93 ARENALES, M.N.; MORABITO, R.N. An and/or graph approach to the solution of two-dimensional non-guillotine cutting problems

Nº 002/93 NICOLETTI, M.C.; MONARD, M.C. Herbrand interpretation model and least model within the framework of logic programming

Nº 001/93 MORABITO, R.; ARENALES, M.N. An and/or graph approach to the container loading problem